

Single inclusive pion p_T -spectra in proton-proton collisions at $\sqrt{s} = 22.4$ GeV: data versus perturbative QCD calculations

François Arleo¹ and David d'Enterria²

¹ *LAPTH*, Université de Savoie, CNRS, BP 110, 74941 Annecy-le-Vieux cedex, France*

² *CERN, PH Dept., 1211 Geneva 23, Switzerland*

We compare the inclusive transverse momentum spectra of single pions above $p_T = 3$ GeV/ c measured in proton-proton (p - p) collisions at $\sqrt{s} = 21.7 - 23.8$ GeV, with next-to-leading order (NLO) perturbative QCD (pQCD) predictions using recent parametrizations of the parton densities and parton-to-pion fragmentation functions. Although the dependence on the theoretical scales is large, the calculations can reproduce the experimental results both in magnitude and shape. Based on the existing data and on a pQCD \sqrt{s} -rescaling of the measured spectra, we provide a practical parametrization of the baseline p - p pion transverse momentum spectrum to be compared to nucleus-nucleus collisions data at $\sqrt{s_{NN}} = 22.4$ GeV.

PACS numbers: 13.85.Ni 12.38.-t 12.38.Bx 13.87.Fh

I. INTRODUCTION

The study of hadron production at large transverse momenta ($p_T \gg \Lambda_{\text{QCD}} \approx 0.2$ GeV) in hadronic interactions is a valuable testing ground of the perturbative regime of Quantum Chromodynamics (pQCD), providing information on both the parton distribution functions (PDFs) in the proton, and the parton-to-hadron fragmentation functions (FFs) [1]. In the last years, a renovated interest in high- p_T hadron production has been driven mainly by studies of “jet quenching” phenomena in high-energy nucleus-nucleus (A-A) collisions [2] as well as of the proton spin structure in polarized p - p collisions [3, 4]. In A-A collisions, the observed large suppression of high- p_T hadron yields compared to (appropriately scaled) p - p cross sections [5, 6] – attributed to parton energy loss due to medium-induced gluon radiation [7, 8] – provides valuable information on the transport properties of hot and dense QCD matter [2]. The energy density at which such “jet quenching” phenomena sets in in A-A collisions can signal the possible transition from a hadronic to a deconfined quark-gluon system. Whereas unambiguous signals of high- p_T hadron suppression have been found at the Relativistic Heavy-Ion Collider (RHIC) in central Au-Au collisions at $\sqrt{s_{NN}} = 200$ GeV [5, 6] and 62.4 GeV [9, 10], one cannot draw any firm conclusion yet at the Super Proton Synchrotron (SPS) energies ($\sqrt{s_{NN}} = 17.3$ GeV) [11] due to the lack of a valid (experimental and/or theoretical) proton-proton reference [12]. Recently, the PHENIX collaboration has presented results on high- p_T neutral pion production in Cu-Cu collisions at energies, $\sqrt{s_{NN}} = 22.4$ GeV, close to the SPS range [13]. We present here an experimental and theoretical study of the pion p_T -spectrum in p - p collisions required in order to determine the associated nuclear “suppression factor”, $R_{AA}(p_T) \propto (dN_{AA}/dp_T)/(dN_{pp}/dp_T)$ in A-A collisions at this center-of-mass (c.m.) energy.

In Section II, we compile and examine all existing experimental spectra for π^0 [14, 15, 16, 17, 18, 19, 20, 21] and π^\pm [21, 22] at c.m. energies in the range $\sqrt{s} = 21.7 - 23.8$ GeV. We notice that most of the data appear to be consistent with each other within uncertainties, despite some spread. In Section III, we compare these data to pQCD calculations at Next-to-Leading Order (NLO) accuracy, as implemented in the Monte Carlo programme INCNLO [23, 24]. We discuss in some detail the improvements in the model predictions thanks to the use of recent FFs [25]. For a choice of renormalization-factorization scales in the low side ($\mu/p_T = 1/3 - 1/2$), the calculations can reproduce the experimental results both in magnitude and shape within the uncertainties associated with the limited knowledge of the parton-to-pion fragmentation functions (FFs) and parton distribution functions (PDFs) in this kinematic range. Finally, a practical parametrization of the p - p pion transverse momentum spectrum at $\sqrt{s} = 22.4$ GeV is provided in Section IV for use as denominator in the determination of the corresponding nuclear modification factor in A-A collisions in the low range of energies accessible at the RHIC collider.

* Laboratoire d'Annecy-le-Vieux de Physique Théorique, UMR5108

II. INCLUSIVE PION SPECTRA IN p - p COLLISIONS AT $\sqrt{s} \approx 22.4$ GEV: EXPERIMENTAL MEASUREMENTS

Table I compiles the 13 measurements found in the literature for neutral [14, 15, 16, 17, 18, 19, 20, 21] and charged [21, 22] pion production at c.m. energies around $\sqrt{s} = 22.4$ GeV at mid-rapidity ($y = 0$, corresponding to laboratory angles $\theta_{\text{lab}} \approx 1$ rad in fixed-target kinematics). The data were measured in the 70's at the CERN Intersecting Storage Rings (ISR) collider as well as in the 80's in various CERN and Fermilab (FNAL) fixed-target experiments. The corresponding data points (adding to a total of ~ 220) have been obtained from the Durham database [26]. Assuming isospin symmetry, the π^0 yield is the same as the $(\pi^+ + \pi^-)/2$ yield, and thus we can use both data sets to get a combined pion reference spectrum. The last column of Table I collects the propagated experimental uncertainties of the measurements as reported in the original publications. Two types of errors are often quoted: (i) those related to energy scale (p_T) uncertainties, and (ii) additional systematic and/or absolute normalization (usually luminosity) errors. The p_T -scale uncertainties have been transformed into an associated absolute cross section uncertainty assuming a local power-law distribution with exponent $n \approx 10$. We have conservatively added all quoted uncertainties in quadrature with the point-to-point errors. We note that at variance with the π^0 spectra measured at $\sqrt{s} \approx 63$ GeV [27], there is no need to account for possible direct- γ contaminations in the oldest “non-resolved” pion spectra since, at the lower c.m. energies considered here, the prompt photon contributions start to be significant only *above* the momentum range ($p_T \gtrsim 6$ GeV/ c) actually reached in the experiments.

Reaction	\sqrt{s} (GeV)	p_{lab}/c (GeV)	Collab./Exp.	Ref.	p_T range (GeV/ c)	# data points	Syst. uncertainties
$pp \rightarrow \pi^0 X$	21.7	250.	FNAL E-063	[14]	0.7 – 2.4	29	30%
$pp \rightarrow \pi^\pm X$	21.7	250.	EHS-NA22	[22]	0.1 – 2.2	45	–
$pp \rightarrow \pi^0 X$	22.8	275.	FNAL E-063	[14]	0.4 – 3.8	16	30%
$pp \rightarrow \pi^0 X$	23.0	280.	CERN-WA70	[15]	4.1 – 6.7	8	16–30%
$pp \rightarrow \pi^\pm X$	23.0	–	Brit.-Scand.	[21]	0.2 – 3.0	17	15%
$pp \rightarrow \pi^0 X$	23.0	284.	FNAL E-063	[14]	0.4 – 4.5	14	30%
$pp \rightarrow \pi^0 X$	23.3	–	R-107	[18]	1.0 – 3.0	21	35%
$pp \rightarrow \pi^0 X$	23.5	–	CCRS	[19]	2.5 – 4.0	17	26%
$pp \rightarrow \pi^0 X$	23.6	–	ACHM	[20]	0.7 – 4.5	19	35%
$pp \rightarrow \pi^0 X$	23.8	300.	FNAL E-063	[14]	0.4 – 3.7	12	30%
$pp \rightarrow \pi^0 X$	23.8	300.	CERN-NA24	[16]	1.25 – 6.0	9	15%
$pp \rightarrow \pi^0 X$	23.8	300.	FNAL-E-268	[17]	1.3 – 4.2	10	5%

TABLE I: Compilation of inclusive pion production data in p - p collisions around $\sqrt{s} = 22.4$ GeV and midrapidity: collision, center-of-mass energy, p_{lab} (for fixed-target experiments), collaboration/experiment name, bibliographical reference, measured p_T range, total number of data points, and associated systematic uncertainties in the measured cross sections.

Figure 1 shows all the measured pion p_T spectra. The full range of cross sections covers more than 12 decades. Unlike with what was observed at $\sqrt{s} \approx 63$ GeV [27], the data taken by the various experiments appear in general quite compatible with each other both in shape and absolute cross sections, within the experimental uncertainties and within the differences expected (at high- p_T) due to the slightly dissimilar c.m. energies of the various measurements (see section IV A). The spectra are characterized by an exponential distribution (with inverse slope ~ 150 MeV) at low- p_T ($p_T \lesssim 1$ GeV/ c), followed by a power-law with exponent ~ 10 , and then a drop at the highest p_T 's when running out of phase-space for particle production, approaching the kinematical limit ($p_T^{\text{max}} = \sqrt{s}/2 = 11$ –12 GeV/ c at midrapidity).

III. INCLUSIVE PION SPECTRA IN p - p COLLISIONS AT $\sqrt{s} \approx 22.4$ GEV: NLO PQCD CALCULATIONS

The inclusive cross section for the production of a single pion, differential in transverse momentum p_T and rapidity y , takes the following form at next-to-leading order (NLO) [24]:

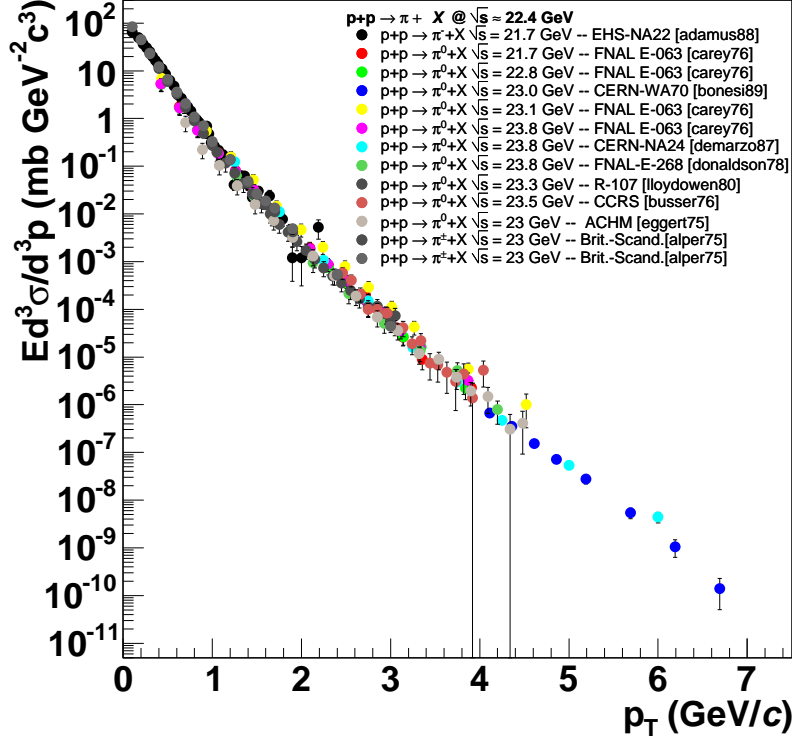


FIG. 1: Compilation of all pion transverse spectra measured in p - p collisions in the range $\sqrt{s} = 21.7 - 23.8$ GeV (see Table I for details).

$$\begin{aligned}
 \frac{d\sigma}{d\mathbf{p}_T dy} = & \sum_{i,j,k=q,g} \int dx_1 dx_2 F_{i/p}(x_1, \mu_F) F_{j/p}(x_2, \mu_F) \frac{dz}{z^2} D_k^\pi(z, \mu_{ff}) \\
 & \times \left[\left(\frac{\alpha_s(\mu_R)}{2\pi} \right)^2 \frac{d\hat{\sigma}_{ij,k}}{d\mathbf{p}_T dy} + \left(\frac{\alpha_s(\mu_R)}{2\pi} \right)^3 K_{ij,k}(\mu_R, \mu_F, \mu_{ff}) \right]. \quad (1)
 \end{aligned}$$

$F_{i/p}$ are the parton distribution functions (PDFs) of the incoming protons p , $D_k^\pi(z, \mu_{ff})$ are the parton-to-pion fragmentation functions (FFs) describing the transition of the parton k into a pion, and $d\hat{\sigma}_{ij,k}/d\mathbf{p}_T dy$ is the Born cross section of the subprocess $i + j \rightarrow k + X$, and $K_{ij,k}$ is the corresponding higher-order term (the full kinematic dependence is omitted for clarity). In this paper, we use the INCNLO program [23] to compute the cross sections, supplemented with various PDFs and FFs sets (see below). The truncation of the perturbative series at next-to-leading order accuracy in α_s , introduces an artificial dependence, with magnitude $\mathcal{O}(\alpha_s^3)$, of the cross section on initial- and final-state factorization scales, μ_F and μ_{ff} , as well as on the renormalization scale μ_R . The choice of scales is to a large extent arbitrary. One often uses as “standard” choice the hard scale of the process, e.g. $\mu_R = \mu_F = \mu_{ff} = p_T$. A more theoretically sound solution is given by using the Principle of Minimum Sensitivity (PMS) [28]. Phenomenological comparisons of pQCD results at various orders (LO, NLO, NNLO) among each other and against various experimental data sets (for charm and beauty, top, Z , W bosons, ...) indicate that choosing a relatively low range of scales $\mu/p_T = 1/3 - 1/2$ provides effectively a reduced sensitivity to higher-order effects [29]. We thus use $\mu_R = \mu_F = \mu_{ff} = p_T/\kappa$, with variation between $\kappa = 2 - 3$. At small p_T and for the scale $p_T/3$, the factorization scale approaches the starting scale Q_0 of the PDF evolution, where the parton densities are not constrained by data. To avoid this problem, we only compute the pion spectra above¹ $p_T = 3$ GeV/ c .

¹ Whenever it becomes smaller than the minimum Q_0 allowed by the PDF or FF parametrization, the hard scale Q is frozen at Q_0 .

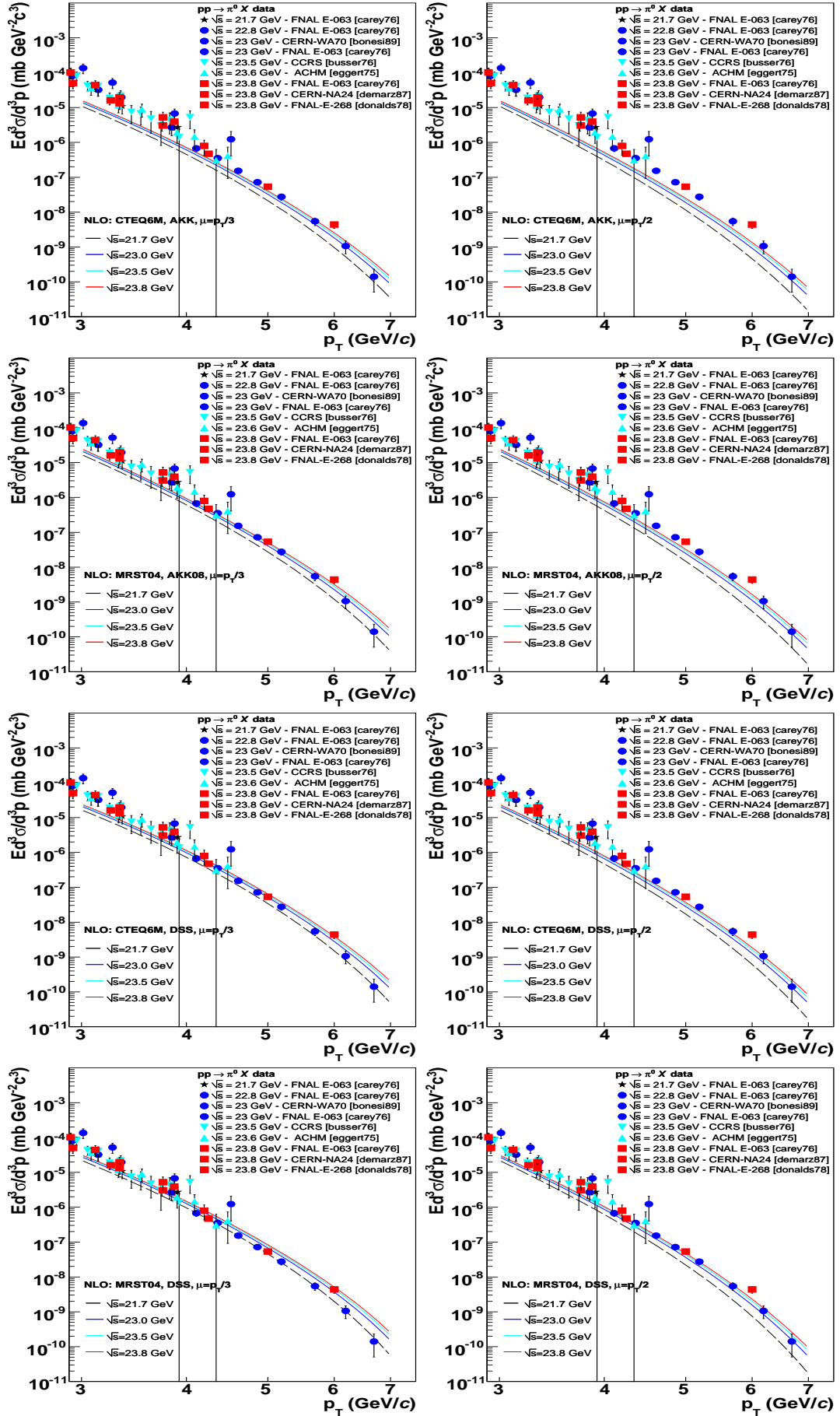


FIG. 2: Comparison of pion transverse spectra measured in p - p collisions at $\sqrt{s} \approx 21.7$ – 23.8 GeV to NLO pQCD predictions. The left (right) plots are for theoretical scales $\mu = p_T/3$ ($p_T/2$). Two sets of PDFs (MRST04 and CTEQ6.1M) and three FFs (AKK05, AKK08, DSS, from top to bottom) are used.

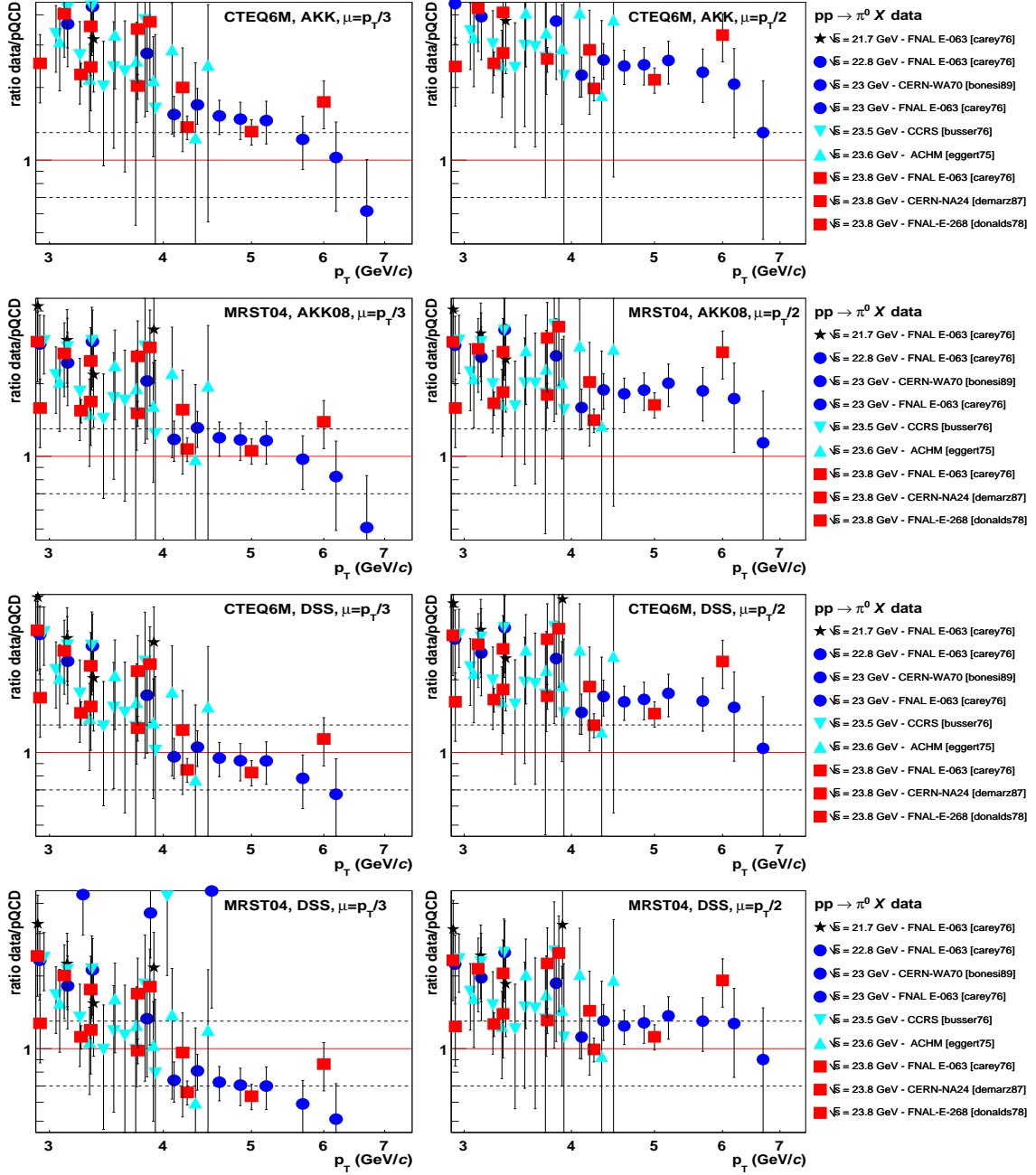


FIG. 3: Ratio of data over pQCD for pion transverse spectra in p - p collisions at $\sqrt{s} \approx 21.7$ – 23.8 GeV. The left (right) plots are for theoretical scales $\mu = p_T/3$ ($p_T/2$). Two sets of PDFs (MRST04 and CTEQ6.1M) and three FFs (AKK05, AKK08, DSS, from top to bottom) are used. The dashed lines are just indicative for variations of $\pm 30\%$ from the reference at $R = 1$.

At large values of p_T , the use of the fixed-order perturbation theory is fully justified, since the perturbative series is controlled by a small expansion parameter, $\alpha_s(p_T^2)$. However, in the typical kinematic range of fixed-target experiments, where $x_T \equiv 2p_T/\sqrt{s} \gtrsim 0.1$, the coefficients of the perturbative expansion are enhanced by extra powers of logarithmic terms of the form $\alpha_s^n \ln^{2n}(1-x_T)$ or $\alpha_s^n \ln^{2n-1}(1-x_T)$. Resummation to all orders of such “threshold” terms – which appear because the initial partons have just enough energy to produce the high-transverse momentum parton – have been carried out at next-to-leading logarithmic (NLL) accuracy in [30, 31]. These studies confirm that accounting for these terms results in a large (approximately p_T -independent) enhancement of the perturbative cross section for pion production in the range of fixed-target energies of relevance here ($\sqrt{s} \approx 20$ GeV). These studies also find that the scale dependence is also reduced at NLL compared to NLO. The

presently used fixed-order calculations (INCNLO) do not include threshold resummations but their effect in the final spectrum is accounted for, in an effective way, by our choice of relatively small theoretical scales, $\mu/p_T = 1/2-1/3$, which results in a cross section increase of a factor of $\sim 2-3$ as compared to the $\mu/p_T = 1/2-2$ range used e.g. in [30, 31].

The two non-perturbative inputs of Eq. (1) are the parton densities and the fragmentation functions. The former are obtained mainly from global-fit analyses of deep-inelastic electron-proton data, the latter from hadron production results in e^+e^- collisions. The PDFs are known to within $\sim 20\%$ uncertainty [32] in the kinematic range of interest here: $x_T = p_T/p_T^{\max} \approx 0.2-0.5$ at midrapidity. We use here two of the latest standard PDFs available: MRST04 [33] and CTEQ6.1M [32]. For the quark and gluon fragmentation functions into pions, we use and compare three parametrizations: the commonly used AKK05 [34] plus two more recent sets: DSS [35] and AKK08 [36]. The dominant fragmentation contribution to Eq. (1) comes from the large- z domain: $\langle z \rangle = \langle p_{\text{hadron}}/p_{\text{parton}} \rangle \approx 0.8$ for $p_T \gtrsim 3$ GeV/ c at $\sqrt{s} = 22.4$ GeV, where the e^+e^- fragmentation data used to obtain the FFs are scarce. In addition, the gluon-to-pion FF is not well determined by e^+e^- annihilation data, as it appears there only at NLO, and we explore small fragmentation scales (in particular, when using $\mu_f = p_T/3$) far away from the kinematical regions where the e^+e^- fits are performed. All these issues, which were a concern for the older FF sets like KKP [37], Kre [38] or AKK05, have been partially solved with the most recent fits [25] which include for the first time also hadronic data (and error analyses, such as for HKNS [39]) in their global analyses. These new fits cover a larger z range and are more sensitive to the gluon fragmentation. As a result, the normalization of the gluon fragmentation function into pions is increased by e.g. up to 50% in AKK08 [36] with respect to AKK05 [34] at the Z^0 mass scale. This has an obvious impact in the absolute normalization of the predicted pion spectra as we discuss below.

In Figs. 2 (spectra) and 3 (ratio data/pQCD), the measured pion p - p single inclusive distributions at various energies are compared to the corresponding NLO predictions for varying theoretical scales ($\mu = p_T/3$ and $p_T/2$), PDFs (MRST04 and CTEQ6.1M) and FFs (AKK05, AKK08 and DSS). In general, the calculations tend to underpredict the measured cross sections. The overall agreement, in the p_T dependence and absolute normalization, improves going from the left (scales $\mu = p_T/3$) to the right (scales $\mu = p_T/2$) and when using MRST instead of CTEQ. The MRST04 parametrization results in a cross section 25% larger than using CTEQ6.1M in the range² $p_T = 3-6$ GeV/ c . Such a difference in the resulting cross sections is larger than expected from error analysis within a single PDF set. The AKK08 and DSS fragmentation functions reproduce better the data than the AKK05 ones. The overall trend is consistent with MRST04 and AKK08/DSS predicting a *higher* pion yield than CTEQ6.1 and AKK05 in the kinematic range of interest here. In any case, the data-theory agreement at fixed-target energies for high- p_T pions is clearly better than for prompt-photon production, where the measured E706 yield at $\sqrt{s} = 31.6-38.6$ GeV appears to be two to three times larger than the corresponding INCNLO predictions [40].

IV. INCLUSIVE PION SPECTRA IN p - p COLLISIONS AT $\sqrt{s} = 22.4$ GEV: A PRACTICAL PARAMETRIZATION

After verifying that the fixed-order pQCD calculations can reproduce relatively well the existing high- p_T pion data at fixed-target energies, the second motivation of this study is to provide a practical parametrization of the p - p pion spectrum at $\sqrt{s} = 22.4$ GeV to be used as reference baseline for high p_T π^0 production in A-A collisions at the same c.m. energy, where no proton-proton data has been yet measured at RHIC [13]. We discuss here the method followed to obtain a fit from the existing experimental data sets after rescaling them to a common center-of-mass energy making use of the NLO predictions.

A. Center-of-mass energy rescaling

The existing data sets (Table I) cover the range of c.m. energies from 21.7 GeV to 23.8 GeV. Although at low- p_T (below ~ 2 GeV/ c), the small differences in \sqrt{s} result into negligible variations of the soft pion yield and all spectra agree well (see Fig. 1), at high p_T – as one approaches the kinematical limit – a couple of GeV of extra c.m. energy available can result into a significant change in the parton-parton cross sections. For instance, as can be seen in Fig. 4,

² However, closer to the kinematical limit, above 8 GeV/ c , the trend changes rapidly and the CTEQ6.1M fit overshoots the MRST04 one by up to 40%, indicating the large current uncertainty of the gluon and sea-quark densities at high values of x .

at $p_T = 5$ GeV/c, going from $\sqrt{s} = 22.4$ GeV up (down) to 23.8 GeV (21.8 GeV) results in an increase (decrease) of the cross section by a factor of $\sim 60\%$ ($\sim 30\%$).

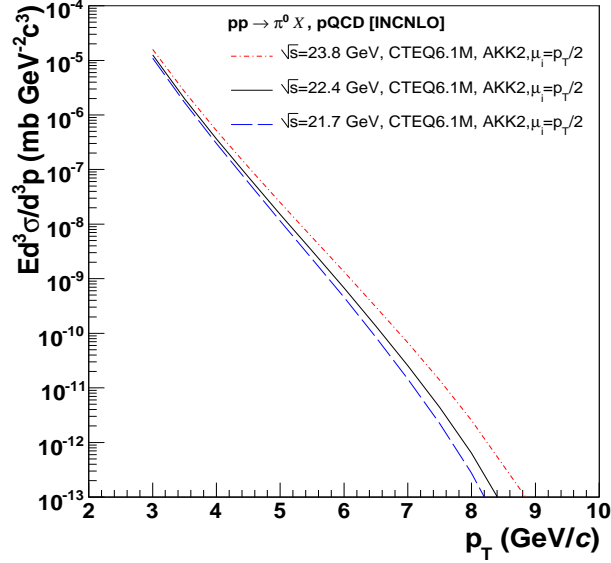


FIG. 4: Differential π^0 cross sections in p - p collisions predicted by NLO pQCD calculations with scales $\mu = p_T/2$, CTEQ6.1M parton-distribution-functions, and AKK08 fragmentation functions at $\sqrt{s} = 21.7, 22.4$ and 23.8 GeV.

Although, as seen in the previous section, there are relatively large uncertainties in the NLO predictions for the *absolute* cross sections, most of these uncertainties cancel out when taking *ratios* of the predicted perturbative yields at different, yet close, c.m. energies. In particular, the (large) scale dependence is completely removed. One can, thus, rescale all experimental data points measured at a given $\sqrt{s} = X$ GeV (in the range 21.8 – 23.8 GeV) to a common $\sqrt{s} = 22.4$ GeV value via the following prescription:

$$\frac{d\sigma_{\text{exp}}(\sqrt{s} = 22.4 \text{ GeV})}{dp_T} = \left(\frac{d\sigma_{\text{NLO}}/dp_T(\sqrt{s} = 22.4 \text{ GeV})}{d\sigma_{\text{NLO}}/dp_T(\sqrt{s} = X \text{ GeV})} \right) \times \frac{d\sigma_{\text{exp}}(\sqrt{s} = X \text{ GeV})}{dp_T}. \quad (2)$$

The pQCD cross-sections are computed in the range $p_T \approx 3$ – 10 GeV/c for the 4 energies under consideration and the ratio over the predictions at $\sqrt{s} = 22.4$ GeV is fitted to a polynomial form of order 2 or 4. Obviously, to minimize the theoretical uncertainties, both the denominator and numerator of the NLO “rescaling factor” (the expression in parentheses in Eq. (2)) need to be computed using consistently the same PDFs, FFs and scales. The scaling factors provided here are obtained averaging over various different choices of these ingredients. The resulting scaling factors differ, in any case, as expected by a very small factor $\pm 5\%$, well covered within the experimental uncertainties alone. The functional form of the rescaling factor is chosen so that the correction is zero at $p_T = 0$ GeV/c, so as to obtain a smooth extrapolation in the low- p_T region. In any case, below $p_T \approx 1$ GeV/c, the correction is (well) below $\sim 5\%$ and, so, the experimental low- p_T points are virtually unmodified as they should be by applying this rescaling procedure. The final correction functions are shown as a function of p_T in Fig. 5.

In order to better estimate the uncertainty of the rescaling factors computed theoretically, the energy rescaling has also been determined *a posteriori*, assuming that the invariant production cross section is a scaling function of $x_T \equiv 2p_T/\sqrt{s}$:

$$E \frac{d^3\sigma(pp \rightarrow \pi X)}{d^3p}(\sqrt{s}) \propto \left(\frac{1}{\sqrt{s}} \right)^4 F(x_T), \quad (3)$$

as it should be in perturbative QCD. Taking for the function F the final parametrization discussed in the next Section, $F(x_T) = (22.4 \text{ GeV})^4 f(x_T \times [11.2 \text{ GeV}])$, the rescaling factor is computed using Eq. (3). The difference between this empirical estimate and the theoretical rescaling factors, roughly 10%, is assigned as the uncertainty of the present energy rescaling procedure.

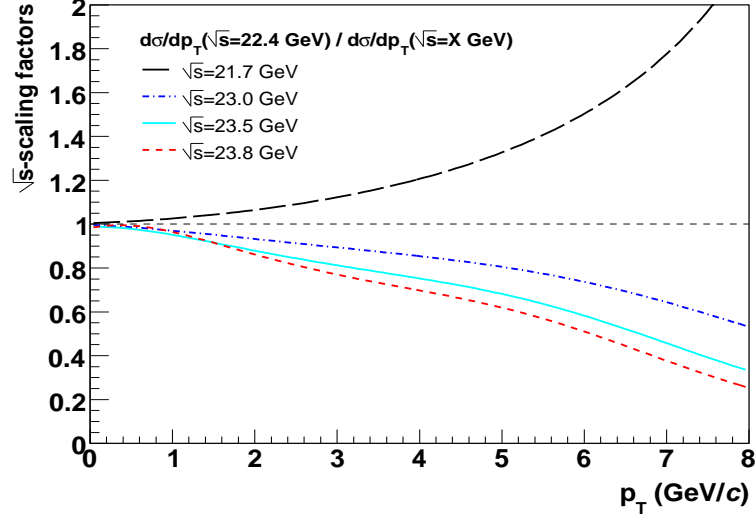


FIG. 5: Rescaling correction factors of the pion cross-sections at c.m. energies 21.7–23.8 GeV to a common $\sqrt{s} = 22.4$ GeV value, as a function of p_T , obtained from the ratio of NLO calculations given by Eq. (2).

B. Global fit of the rescaled pion p_T spectra at $\sqrt{s} = 22.4$ GeV

By applying the appropriate energy correction factors discussed in the previous section to all the experimental data sets, we obtain a new set of data points which approximates better the expected π^0 spectrum at $\sqrt{s} = 22.4$ GeV. The experimental spectrum $\left. \frac{Ed^3\sigma}{d^3p} \right|_{y=0}$ is fitted to the following empirical 4-parameter functional form:

$$f(p_T, \{p_i\}_{i=0,3}) = p_0 \cdot [1 + (p_T/p_1)]^{p_2} \cdot [1 - (p_T/p_T^{\max})]^{p_3} \quad (4)$$

Such a formula interpolates well between the low- p_T exponential shape and the high- p_T power-law while fulfilling the requirement of being zero at the kinematical limit ($p_T^{\max} = 11.2$ GeV/c, fixed in the fit). The p_0 parameter gives the cross-section at zero p_T , p_1 indicates the transition value from soft to hard production, and the p_2 and p_3 exponents characterize the power-law and end of phase-space ranges. After rejecting two data sets which are not consistent with the rest of spectra (see below), we obtain a final set of $n_{\text{dat}} = 194$ data points fitted with Eq. (4). The resulting fit is shown in Fig. 6. The parameters are obtained from the minimization of the χ^2 function

$$\chi^2(\{p_i\}) = \sum_{j=1}^{n_{\text{dat}}} \left[\frac{\left. \frac{Ed^3\sigma}{d^3p} \right|_{y=0}(p_{T_j}) - f(p_{T_j}, \{p_i\})}{\sigma_j} \right]^2, \quad (5)$$

where σ_j is the statistical and systematic error of point j added in quadrature. The error of the parameters p_i are given from a deviation of $\Delta\chi^2$ from its minimum:

$$\chi^2(\{p_i + \delta p_i\}) - \chi^2(\{p_i\}) = \Delta\chi^2. \quad (6)$$

Although a usual choice is $\Delta\chi^2 = 1$, we shall conservatively allow for a larger variation of the fit parameters assuming $\Delta\chi^2 = 50$ in what follows³, similarly to what is done in global fit analyses of parton densities or fragmentation functions (see e.g. [35, 41]). From this procedure, the corresponding parameters are:

$$\begin{aligned} p_0 &= 176.3 \pm 69.7 \text{ [mb GeV}^{-2} \text{c}^3] \\ p_1 &= 2.38 \pm 1.19 \text{ [GeV/c]} \\ p_2 &= -16.13 \pm 7.21 \\ p_3 &= 6.94 \pm 5.64 \\ \chi^2/\text{ndf} &= 208.2/190 \end{aligned} \quad (7)$$

³ This would correspond to an increase of 25% of $\chi_{\text{min}}^2/\text{ndf}$ with $\text{ndf} \simeq 200$.

with an important correlation between parameters and errors, as indicated by the large non-diagonal terms of the covariance (error) matrix, V_{ij} :

$$V_{ij} = \begin{pmatrix} 1.000 & -0.725 & -0.603 & 0.394 \\ -0.725 & 1.000 & 0.981 & -0.862 \\ -0.603 & 0.981 & 1.000 & -0.940 \\ 0.394 & -0.862 & -0.940 & 1.000 \end{pmatrix}$$

Note that at low p_T , this fit is consistent with an exponentially decreasing function with inverse slope $-p_1/p_2 = 148 \pm 16$ MeV. The scale p_1 , which naively separates soft from hard dynamics, has a sensible value ~ 2 –3 GeV. Finally, the negative power slope, $p_2 = -16.13$, is found to be larger in absolute value than $p_2 = -10$ obtained at $\sqrt{s} = 200$ GeV [42]. This is expected from the steeper dependence of parton densities and fragmentation functions probed at higher x and z , respectively, at lower \sqrt{s} . The uncertainty Δf of the fit is given by

$$\Delta f = \left[\sum_{i,j=0}^3 \frac{\partial f}{\partial p_i} V_{ij} \frac{\partial f}{\partial p_j} \right]^{1/2}. \quad (8)$$

The relative uncertainty of the parametrization, $\Delta f/f$, spans the range from $\sim 15\%$ at low $p_T \lesssim 2$ GeV/ c up to 25% (40%) at $p_T = 4$ GeV/ c (5 GeV/ c) in the range covered by the RHIC measurements [13]. At higher p_T 's the fit is completely unconstrained due to the lack of data, and its uncertainty is very large.

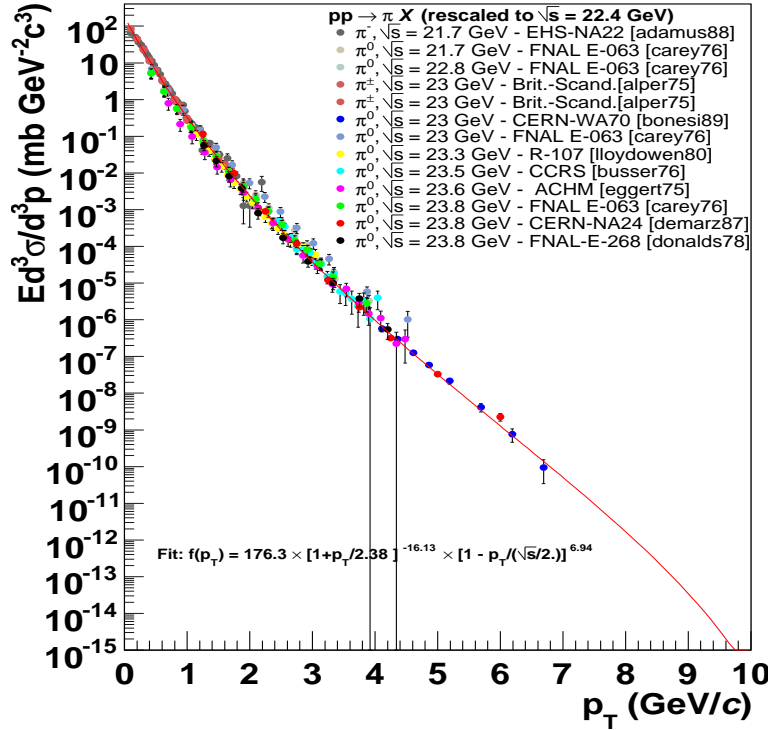


FIG. 6: Compilation of all pion transverse spectra measured in p - p collisions at $\sqrt{s} = 21.7 - 23.8$ GeV, rescaled to a common $\sqrt{s} = 22.4$ GeV energy, as discussed in the text, and fitted to Eq. (4), with the parameters (7).

Figure 7 shows the ratio of all data sets compiled and rescaled in this work over the fit Eq. (4) with the parameters quoted above. All data sets – but Carey76 [14] at $\sqrt{s} = 23$ GeV and Eggert75 [20] at $\sqrt{s} = 23.6$ GeV which have a shape and absolute normalization inconsistent with the rest of measurements and have not been included in the final global analysis – show a rather good agreement with the proposed parametrization, as also indicated by $\chi^2/\text{ndf} \simeq 1.1$. We note that our empirical fit includes also the low- p_T range, not amenable to perturbative analysis, since we want to provide a (potentially useful) p - p reference parametrization in the whole range covered by the nucleus-nucleus data.

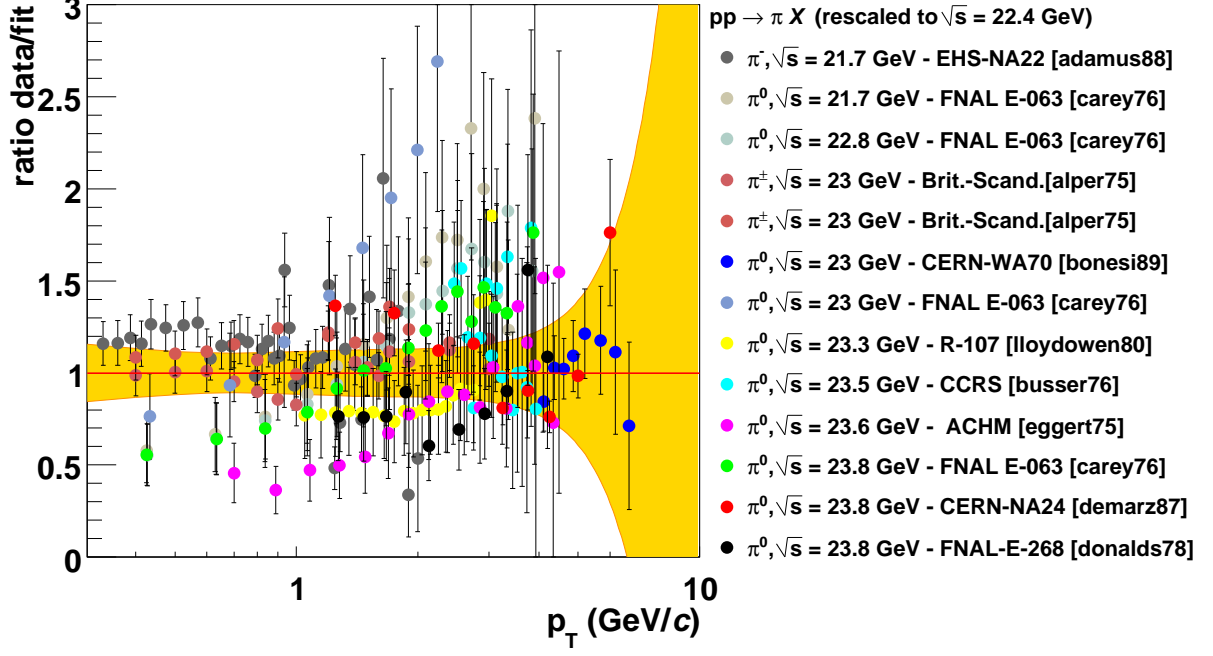


FIG. 7: Ratio of all pion transverse spectra measured in p - p collisions rescaled to $\sqrt{s} = 22.4$ GeV over the fit given by Eq. (4) with the parameters (7). The yellow band represents the uncertainty assigned to the parametrization, as given by Eq. (8). The [carey76] and [eggert75] points at $\sqrt{s} = 23.6, 23.$ GeV respectively [14, 20] have been excluded from the global fit.

V. SUMMARY

We have compared the available high- p_T pion spectra measured in proton-proton collisions in the range $\sqrt{s} = 21.7 - 23.8$ GeV (CERN-ISR collider and CERN and FNAL fixed-target) to next-to-leading order pQCD calculations with recent parton distribution functions (PDFs) and fragmentation functions (FFs). A choice of the theoretical (factorization, fragmentation and normalization) scales between $p_T/3$ and $p_T/2$ reproduces well the magnitude and shape of the experimental data. CTEQ6.1 and MRST04 parton densities yield results different by up to 25%. Second-generation parton-to-pion fragmentation functions (FFs) with updated constraints on the gluon and large- z fragmentation region such as DSS or AKK08, improve the agreement of the data with the calculations compared to older FF parametrizations.

A baseline nucleon-nucleon reference p_T -distribution for inclusive π^0 production at $\sqrt{s} = 22.4$ GeV has been determined from a global fit analysis of the available data. The measured (high- p_T) data sets have been rescaled at a common c.m. energy making use of the predicted NLO pQCD yields at the various \sqrt{s} . The resulting parametrization is consistent within $\pm 15\%$ and $\pm 40\%$ systematic uncertainty with the rescaled π^0 and π^\pm measurements at low ($p_T \lesssim 2$ GeV/ c) and moderate ($p_T \simeq 5$ GeV/ c) transverse momentum. Such a reference – Eq. (4) with fit parameters (7) – can be used in order to obtain the nuclear modification factor of high- p_T pion production in A-A collisions at $\sqrt{s_{NN}} = 22.4$ GeV measured at RHIC.

Acknowledgments

Valuable comments and discussions with Klaus Reygers and Mike J. Tannenbaum are acknowledged. We thank Simon Albino for providing us with the latest AKK08 fragmentation functions. DdE is supported by the 6th EU Framework Programme (contract MEIF-CT-2005-025073). FA thanks the hospitality of CERN PH-TH department where part

of this work has been completed.

-
- [1] W. M. Geist, D. Drijard, A. Putzer, R. Sosnowski and D. Wegener, Phys. Rep. **197**, 263 (1990).
 - [2] D. d’Enterria, “Jet quenching in High-Energy Heavy-Ion Collisions”, Landolt-Boernstein Series (Springer-Verlag, Berlin, to be published).
 - [3] G. Bunce, N. Saito, J. Soffer and W. Vogelsang, Ann. Rev. Nucl. Part. Sci. **50**, 525 (2000)
 - [4] B. Jager, A. Schafer, M. Stratmann and W. Vogelsang, Phys. Rev. D **67** (2003) 054005.
 - [5] S. S. Adler *et al.* [PHENIX Collaboration], Phys. Rev. Lett. **91**, 072301 (2003)
 - [6] J. Adams *et al.* [STAR Collaboration], Phys. Rev. Lett. **91** 172302 (2003)
 - [7] R. Baier, D. Schiff, and B.G. Zakharov, Ann. Rev. Nucl. Part. Sci. **50** 37 (2000).
 - [8] M. Gyulassy, I. Vitev, X. N. Wang and B. W. Zhang, arXiv:nucl-th/0302077.
 - [9] T. Isobe, Acta Phys. Hung. A **27**, 227 (2006)
 - [10] B. I. Abelev *et al.* [STAR Collaboration], Phys. Lett. B **655**, 104 (2007)
 - [11] C. Blume, Nucl. Phys. A **783** (2007) 65, and references therein.
 - [12] D. d’Enterria, Phys. Lett. B **596**, 32 (2004)
 - [13] A. Adare *et al.* [PHENIX Collaboration], Phys. Rev. Lett. **101**, 162301 (2008).
 - [14] D. C. Carey *et al.*, Phys. Rev. D **14**, 1196 (1976).
 - [15] M. Bonesini *et al.* [WA70 Collaboration], Z. Phys. C **38**, 371 (1988).
 - [16] C. De Marzo *et al.* [NA24 Collaboration], Phys. Rev. D **36**, 8 (1987).
 - [17] G. Donaldson *et al.*, Phys. Lett. B **73**, 375 (1978).
 - [18] D. Lloyd Owen *et al.*, Phys. Rev. Lett. **45**, 89 (1980).
 - [19] F. W. Busser *et al.*, Nucl. Phys. B **106**, 1 (1976).
 - [20] K. Eggert *et al.*, Nucl. Phys. B **98**, 49 (1975).
 - [21] B. Alper *et al.* [British-Scandinavian Collaboration], Nucl. Phys. B **100**, 237 (1975).
 - [22] M. Adamus *et al.* [EHS-NA22 Collaboration], Z. Phys. C **39**, 311 (1988).
 - [23] P. Aurenche, T. Binoth, M. Fontannaz, J.-P. Guillet, G. Heinrich, E. Pilon and M. Werlen, http://lappweb.in2p3.fr/lapth/PHOX_FAMILY/readme_inc.html
 - [24] P. Aurenche, M. Fontannaz, J. P. Guillet, B. A. Kniehl and M. Werlen, Eur. Phys. J. C **13**, 347 (2000)
 - [25] S. Albino *et al.*, arXiv:0804.2021 [hep-ph] and references. therein.
 - [26] <http://durpdg.dur.ac.uk/HEPDATA/>
 - [27] D. d’Enterria, J. Phys. G **31**, S491 (2005).
 - [28] P.M. Stevenson, Phys. Rev. **D23** (1981) 2916;
P.M. Stevenson, H.D. Politzer, Nucl. Phys. **B277** (1986) 758;
P. Aurenche, R. Baier, M. Fontannaz, D. Schiff, Nucl. Phys. **B286** (1987) 509.
 - [29] A. Geiser, Proceeds. Photon’07, Paris, Nucl. Phys. **B Proc. Suppl.**, to appear.
 - [30] D. de Florian and W. Vogelsang, Phys. Rev. D **71** (2005) 114004
 - [31] D. de Florian, W. Vogelsang and F. Wagner, Phys. Rev. D **76**, 094021 (2007).
 - [32] J. Pumplin *et al.* [CTEQ Collaboration], J. High Energy Phys. **0207**, 012 (2002).
 - [33] A. D. Martin, R. G. Roberts, W. J. Stirling and R. S. Thorne, Phys. Lett. B **604** (2004) 61.
 - [34] S. Albino *et al.*, Nucl. Phys. **B725** (2005) 181; Nucl. Phys. **B734** (2006) 50
 - [35] D. de Florian, R. Sassot and M. Stratmann, Phys. Rev. D **75**, 114010 (2007).
 - [36] S. Albino, B. A. Kniehl and G. Kramer, Nucl. Phys. **B803** (2008) 42.
 - [37] B. A. Kniehl, G. Kramer and B. Pötter, Nucl. Phys. **B582**, 514 (2000)
 - [38] S. Kretzer, Phys. Rev. **D62**, 054001 (2000).
 - [39] M. Hirai, S. Kumano, T. H. Nagai and K. Sudoh, Phys. Rev. **D75** (2007) 094009.
 - [40] P. Aurenche, M. Fontannaz, J. P. Guillet, E. Pilon and M. Werlen, Phys. Rev. D **73** (2006) 094007
 - [41] J. Pumplin *et al.*, Phys. Rev. **D65** (2001) 014013.
 - [42] S. S. Adler *et al.* [PHENIX Collaboration], Phys. Rev. Lett. **91** (2003) 241803.